Salgado, C. et al., 2020. Functional properties of photo-crosslinkable biodegradable polyurethane nanocomposites. Polymer degradation and stability, 178, pp.Polymer degradation and stability, August 2020, Vol.178.

Available at https://doi.org/10.1016/j.polymdegradstab.2020.109204

Functional properties of photo-crosslinkable biodegradable polyurethane nanocomposites

Cástor Salgado, Marina P. Arrieta, Valentina Sessini, Laura Peponi, Daniel López, Marta Fernández-García

PII: S0141-3910(20)30136-1

DOI: https://doi.org/10.1016/j.polymdegradstab.2020.109204

Reference: PDST 109204

To appear in: *Polymer Degradation and Stability*

Received Date: 31 October 2019

Revised Date: 1 April 2020

Accepted Date: 20 April 2020

Please cite this article as: Salgado Cá, Arrieta MP, Sessini V, Peponi L, López D, Fernández-García M, Functional properties of photo-crosslinkable biodegradable polyurethane nanocomposites, *Polymer Degradation and Stability* (2020), doi: https://doi.org/10.1016/j.polymdegradstab.2020.109204.

Credit Author Statement:

Conceptualization: L.P. M.F.-G.; Data curation: C.S. M.A. V.S.; Funding acquisition: L.P. D.L. M.F.-G.; Investigation: C.S. M.A. V.S.; Methodology; Supervision; Roles/Writing - original draft C.S. M.A. V.S. L.P; Writing - review & editing C.S. M.A. V.S. L.P. M.F-G. D.L.

Functional properties of photo-crosslinkable biodegradable polyurethane nanocomposites

Cástor Salgado[1], Marina P. Arrieta[1], Valentina Sessini[1,2], Laura Peponi[1,3]*, Daniel López[1,3], Marta Fernández-García[1,3]*

1. Instituto de Ciencia y Tecnología de Polímeros (ICTP-CSIC), C/ Juan de la Cierva 3, 28006 Madrid, Spain
2. Laboratory of Polymeric and Composite Materials, University of Mons – UMONS, Place du Parc 23, 7000 Mons, Belgium
3. Interdisciplinary Platform for Sustainable Plastics towards a Circular Economy-Spanish National Council (SusPlast-CSIC), Madrid, Spain

Corresponding author: lpeponi@ictp.csic.es, martafg@ictp.csic.es

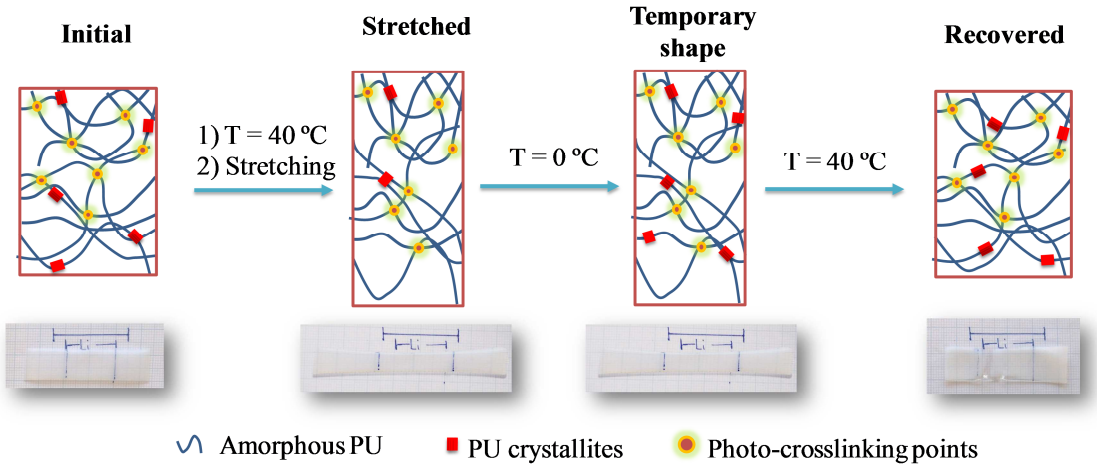

Keywords: Polyurethane, coumarin, photo-crosslinking, swelling, shape-memory, biodegradable.

Abstract

Smart and functional properties of coumarin and PCL-based polyurethane (PU) nanocomposites reinforced with both pristine silica nanoparticles and silica nanoparticles modified with coumarin, have been studied. Coumarin is a photo-responsive derivative, which induces photo-crosslinking when it is incorporated in the PU moieties. Swelling measurements were performed to study the photo-crosslinking fraction and the results are in concordance with the degree of crosslinking (DC) calculated by UV measurements. Shape memory behavior was studied by thermo-mechanical cycles, by measuring the strain recovery and shape fixity ratios of the photo-crosslinked films. The modification of silica nanoparticles allows an improvement in the dispersion of the reinforcements into the PU matrix, which leads to an enhancement of the shape memory properties. Finally, the materials were disintegrated under composting conditions at laboratory scale level to confirm their biodisintegrable behavior.

1. Introduction

Coumarin derivatives are systems commonly used in photo-chemistry owing to its capability to assemble dimers under the effect of UV irradiation [1-4]. Coumarin molecules reach a [2π+2π] cycloaddition photo-reaction with itself, in which the lactone double bond of one coumarin reacts with another one to arrange a 4-carbon ring. The dimerization of coumarin is a reversible process, in which the photo-dimerization is usually activated above 300 nm and the photo-cleavage is a shorter duration process activated below 300 nm [5]. These properties lead to coumarin as one of the most used systems in the development of photo-responsive polymers [1, 6-8]. Furthermore, poly(ε-caprolactone) diol (PCL) is a biodegradable polymer with good physical properties such as high elongation at break or low crystallinity, widely used for flexible film production. PCL is used as soft segment in the synthesis of polyurethanes (PUs) in order to obtain materials with optimal elasticity, tensile strength, transparency or low toxicity [9-13]. Several applications of PUs as biomedical devices [14], tissue engineering materials [15],

gas-separation membranes [16], films for food packaging [13, 17] or surface coatings [18-21] have been reported. Furthermore, inorganic nanofillers are typically used to reinforce PUs and to obtain nanocomposites with enhanced performance for specific applications. Besides, nanoparticles can be functionalized to achieve better interaction with the polymeric matrix [22], leading to an improvement on its physico-chemical properties [23]. PCL-based PUs have shown good compatibility with inorganic reinforcements [12, 24, 25], for example with silica nanoparticles (SiNPs), deeply used for its low cost, high surface area, hardness, chemical stability and high thermal resistance [26, 27].

Moreover, the formation of a PU network can be revealed by a gelation process, in which a crosslinked polymer is able to soak up water or organic solvents into their internal network. A polymer gel can form a soft and wet surface when it is swollen. Gelation or swelling behavior depends on the stoichiometry, functionality, kind of solvent or temperature [28, 29]. The use of coumarin moieties in the formation of gels has been explored due to its intrinsic photo-crosslinking behavior [30, 31]. The crosslinking degree of polyurethane elastomers can be reached by swelling measurements in numerous organic solvents [32].

In addition, PUs are widely used as smart materials in self-healing approach as well as in shape memory applications. In particular, shape memory behavior consists in the capability of the material to fix a temporary shape and to recover its initial shape upon the application of an external stimulus, like temperature [33], humidity [34], pH [35] or light [36] among others. In thermally-activated shape memory polymers, the activation usually takes place at a transition temperature that could be the glass transition (T_g) or the melting temperature (T_m) [37]. PUs are able to undergo shape-memory behavior owing to their phase separation morphology, in which the different chemical interaction between hard (HS) and soft (SS) segments produces two active phases [13]. The fixity phase (HS) is responsible to recover the original shape of the material, meanwhile the switching phase (SS) is the responsible of fixing the temporary shape. The relation between HS and SS determines the microstructural morphology in the PU matrix and

therefore, can modify its shape memory behavior [38]. Several strategies are reported in the literature to improve the shape memory properties of PUs by developing either chemical or physical modifications, such as the adjustment of hard-to-soft segment ratio [39], the incorporation of crosslinking networks [40], or the addition of inorganic nanoparticles, among others [41]. In this sense, it has been shown that the capability to fix the temporary shape of PCL-based PUs can be improved by the development of composites [13, 42] and/or nanocomposites [43, 44].

The use of biodegradable polymers is a current trend carried out because of the considerable accumulation of plastic wastes in the environment after their useful life. The use of PCL-based PUs in the industrial sector is triggered by their upright behavior as film or coatings [18, 19]. PCL-based PUs can be disintegrated under composting conditions, which starts through a hydrolytic degradation process, followed by the scission of the polymer chains, which are susceptible for a further microorganism attack [13, 45].

In our previous work, PCL and coumarin-based photo-crosslinkable PUs were synthesized [20] and further reinforced with neat SiNPs [19] as well as with coumarin-modified silica nanoparticles, mSiNPs [21] studying their photo-crosslinkage by UV irradiation as well as their mechanical and thermal properties. In the present work, the best formulations of those PUs and both SiNPs and mSiNPs nanocomposites were selected and photo-crosslinked by UV irradiation at 365 nm. These materials were here swelled to study their crosslinking fraction, which was compared with the degree of crosslinking (DC) previously obtained by UV measurements [21]. Moreover, with the main objective to evaluate the possibility to use these materials as smart thermally-activated shape memory coatings, in this work thermo-mechanical cycles were performed to study their shape memory properties. Finally, the nanocomposites were biodisintegrated under composting conditions to corroborate their sustainable end-life option.

2. Materials and Methods

2.1 Materials

2,2-Bis(hydroxymethyl)propionic acid, p-toluenesulfonic acid (PTSA), 1,4-dioxane, 2,2-dimethoxypropane, N,N'-dicyclohexylcarbodiimide (DCC), dichloromethane (DCM), ethyl acetoacetate, resorcinol, 2-bromoethanol, ethyl acetate, 4-(dimethylamino)pyridine (DMAP), triethylamine (TEA), potassium carbonate, Dowex H^+ resin, poly(ε-caprolactone) diol (M_n=530 g mol^{-1}), poly(ε-caprolactone) diol (M_n=2000 g mol^{-1}), stannous octoate ($Sn(Oct)_2$), hexamethylene diisocyanate (HDI), 1,2-dichloroethane (DCE), N,N-dimethylformamide (DMF), HPLC grade lithium bromide (LiBr) and (3-aminopropyl)triethoxysilane (APTES) were supplied by Sigma-Aldrich. Acetone, DMF, *n*-hexane, chloroform, ethanol and methanol, were supplied by Scharlau. Sulfuric acid (98%), ammonia (30%) and sodium chloride were supplied by Panreac. Sodium bisulfate and succinic anhydride were supplied by Fluka and anhydrous magnesium sulfate ($MgSO_4$) was supplied by Quality Chemicals. Thin liquid chromatography (TLC) silica gel 60 F_{254} aluminum sheets (20×20 cm) were purchased from Merck. Fumed silica dioxide nanopowder (primary particle average size: 7-14 nm) was purchased from Interchim Innovations. All the products were used as received.

2.2 Synthesis of nanocomposites

PCL and coumarin-based PUs were obtained as described in a previous work [20]. The synthesis is showed in the **Scheme 1**. In brief, coumarin diol (CD) was synthesized according to the synthesis of Seoane-Rivero et al. [46]. Equimolar amounts (0.1 eq) of CD and hexamethylene diisocyanate (HDI) were dissolved in 20 mL of DCE at 80 ºC. After 2 hours of mixing, the pre-polymer was reacted with a solution of PCL (0.9 eq.), HDI (0.9 eq.) and $Sn(Oct)_2$ (20 μL) in 20 mL of DCE and stirred at 100 ºC. The reaction end was followed by FTIR until the -NCO group band (2270 cm^{-1}) disappears. The mixture was poured into PTFE round molds, until the solvent

was evaporated. The obtained films showed thickness in the range of 200-250 μm and they were allowed to dry at vacuum for 10 hours before characterization.

Non-reinforced PUs were characterized as obtained from the synthesis. Meanwhile, the samples reinforced with coumarin-modified and unmodified fumed silica nanoparticles were prepared by following the procedure described in previous works [19, 21]. Briefly, modification of silica nanoparticles was achieved by reacting fumed silica, (3-aminopropyl)triethoxysilane and a coumarin derivative.

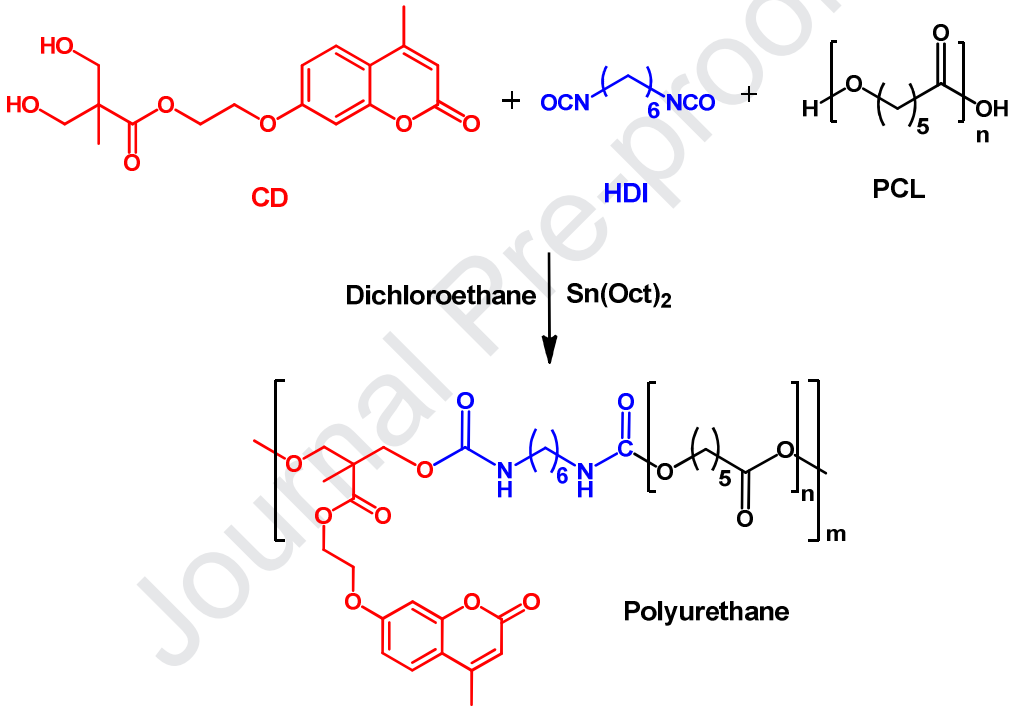

Scheme 1. Synthesis of PU-based on PCL and coumarin.

Finally, the samples were photo-crosslinked throughout 90 minutes on both sides of the film using a CL-1000 Ultraviolet Crosslinker (UVP-Madrid, Spain) at 365 nm with 5×8 W (maximum UV energy exposure setting of 999,900 μJ/cm^2). All the samples studied in this work are summarized in **Table 1**.

Table 1. Collects the samples used in this work.

PCL (Mn)	Coumarin (% mol)	SiNPs (wt %)		Modified SiNPs (wt %)
		0	1	1
530	5	PU530CD5	PU530CD5-Si1	PU530CD5-mSi1
2000	0	PU2K		
	5	PU2KCD5	PU2KCD5-Si1	PU2KCD5-mSi1

2.3 Swelling behavior

Swelling measurements were conducted by following the procedure shown in the **Scheme 2**. Photo-crosslinked PU films were cut in a rectangular shape (1 cm × 0.5 cm), weighted (W_0) and stirred at 60 rpm in a flask with 3 mL of chloroform for 24h at room temperature. Then, the solvent was replaced until an equilibrium weight was reached (W_1) and the swelled PUs were dried for 24h at 40 ºC and weighted again (W_2) to determine the crosslinking fraction (CF). Three replicates were measured for each sample.

The swelling degree was obtained by following the **Equation 1** [47]:

$$Sw\ (\%) = \frac{W_1 - W_0}{W_0} x100 \quad \textbf{(1)}$$

W_1 is the weight of swelled material and W_0 is the initial weight.

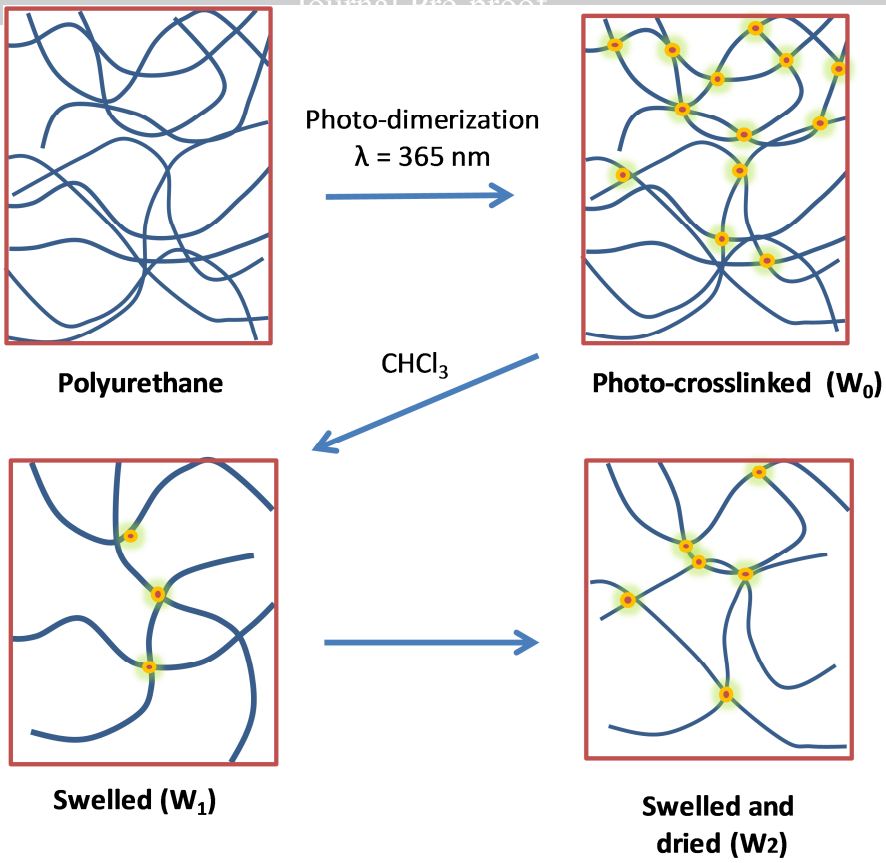

Scheme 2. Depiction of the swelling study for photo-crosslinked PU-based nanocomposites.

The crosslinking fraction was obtained by following the **Equation 2** [48, 49]:

$$CF\ (\%) = \frac{W_2}{W_0} x100 \qquad \textbf{(2)}$$

W_2 is the weight of swelled material after drying.

These results were compared with the degree of crosslinking of nanocomposites previously calculated [19-21] by measuring the decrease of the absorption band of coumarin at 320 nm and using the **Equation 3**:

$$DC\ (\%) = \frac{A320_0 - A320_t}{A320_0} x100 \qquad \textbf{(3)}$$

2.4 Shape memory characterization

To perform the shape memory analysis, first of all, the thermal properties of the samples were studied in order to choose the right transition temperature (T_{trans}) and fixing temperature (T_{fix}) to be used for the thermo-mechanical cycles. Differential Scanning Calorimetry (DSC)

measurements were performed using a TA Instruments DSC Q2000 (New Castle, DE, USA) under nitrogen atmosphere (50 mL/min). The samples were placed in sealed aluminum pans and heated from -80 to 90 ºC at a heating rate of 10 ºC/min. The thermal properties were taken from the DSC first heating scan in order to study the properties of the material as used for the shape memory measurement and simulating the potential application of the materials without any added thermal treatment after processing. The thermally-activated shape memory properties were studied by thermo-mechanical cycles. The measurements were carried out in a Dynamic Mechanical Thermal Analyzer (DMTA Q800) from TA Instruments in film tension mode with controlled force. The samples were cut from casted films of photo-crosslinked PU nanocomposites with rectangular shape of 6 mm × 2.5 mm × 0.2 mm. The samples were submitted to a cycle composed by different steps. In the programming step, the samples were first equilibrated at 40 °C for 5 min in order to melt the PCL-based crystalline phase and then, they were stretched until 50% of strain, applying a tensile stress ramp with a rate of 0.05 MPa/min. Afterwards, the sample was cooled down at 1 ºC/min to 0 ºC (T_{fix}) to promote the crystallization of PCL maintaining the same temperature for 10 min to ensure the maximum PCL crystallization and, consequently, a good fixation of the temporary shape. The stress is finally released at 0.05 MPa/min to 0 MPa and the temperature was maintained for another 15 min to evaluate the real fixity ratio of the samples. Finally, in the recovery step, a temperature ramp was applied at 3 ºC/min to 40 ºC to activate the recovery of the original shape and the temperature was maintained for 30 min to achieve the equilibrium and consequently the maximum strain recovery ratio values. A resumed process is showed in the **Scheme 3** as well as the visual appearance of a film sample of PU2KCD5 during the thermally activated shape memory process.

The strain recovery ratio has been calculated from the **Equation 4**:

$$R_r(N) = \frac{\varepsilon_m - \varepsilon_p(N)}{\varepsilon_m - \varepsilon_p(N-1)} x100 \quad \textbf{(4)}$$

Meanwhile, the capability of the material to recover the temporary shape is defined by the strain fixity ratio, that is calculated from the **Equation 5**:

$$R_f(N) = \frac{\varepsilon_u(N)}{\varepsilon_m} x100 \quad \textbf{(5)}$$

Where ε_m is the deformed strain, ε_p is the recovered strain and ε_u the fixed strain [34].

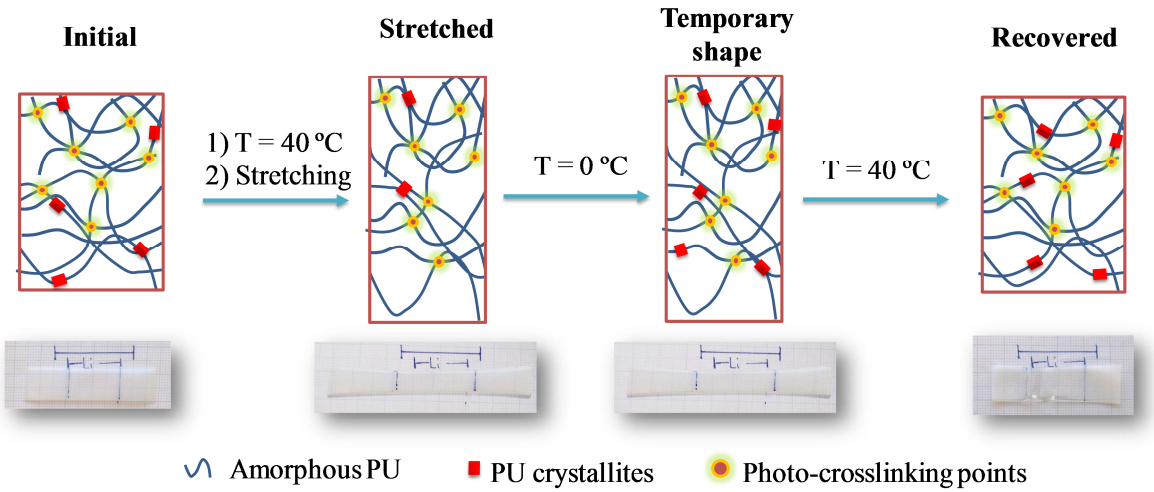

Scheme 3. Evolution of the shape memory process studied for the PU nanocomposites.

2.5 Disintegration under composting conditions

PU-based films and nanocomposites were disintegrated under composting conditions at laboratory scale level according to the ISO 20200 standard [50]. The samples (15 mm × 15 mm × 0.15 mm) were dried and weighed and then they were buried inside a textile mesh (to allow the removal of the disintegrated samples and also the access of the microorganisms and moisture) [51] at 4-6 cm depth in pricked plastic containers, which contained a solid synthetic wet waste prepared with 10% of compost (Mantillo, Spain), 30% rabbit food, 10% starch, 5% sugar, 1% urea, 4% corn oil, 40% sawdust and about 50 wt% of water content. Containers were incubated at aerobic conditions at 58 ºC. Film samples were recovered at 1, 7 and 10 days of disintegration, washed with distilled water, dried firstly in an oven at 37 ºC for 24 h and then under vacuum, and finally reweighed. A qualitative check of the physical disintegration in compost was followed by taken photographs as time-related, while the degree of disintegrability was calculated by normalizing the sample weight at each time to the initial value. Finally, the structural and chemical changes during composting were studied by SEM and FTIR spectroscopy.

3. Results and discussion

Considering that the crosslinked materials has been obtained by irradiation with UV light and this is a superficial treatment, PUs were studied by swelling measurements in chloroform to evaluate the efficiency of crosslinking after the irradiation process at 365 nm in the overall material. Several pictures of the PUs were taken after the photo-crosslinking process. The measurements were performed in two steps: in the first one, the irradiation and subsequent swelling caused a deformation of the films (as seen in **Fig. 1**), which is indicative of an irregular photo-crosslinking process that will be discussed later.

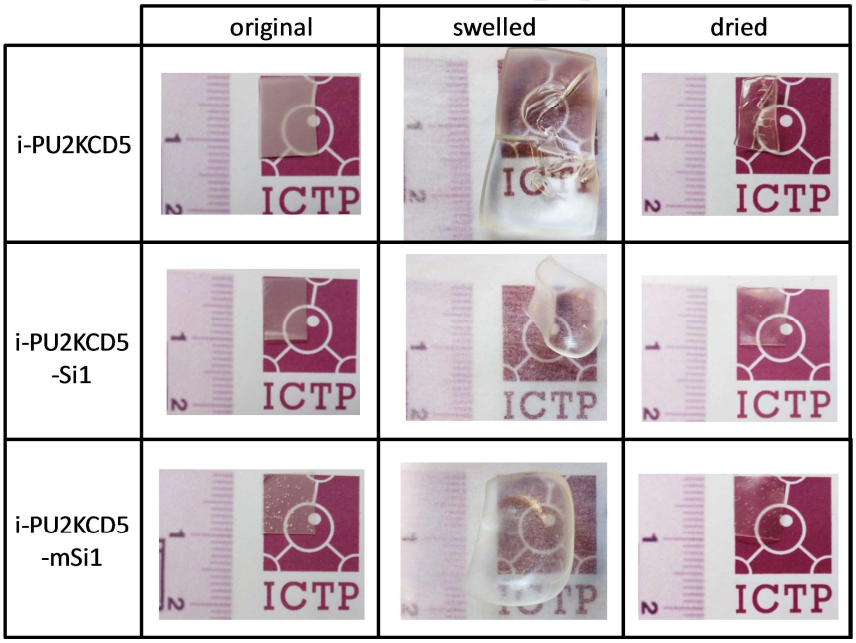

Fig. 1. Visual appearance of PU films before and after swelling measurements.

Afterwards, the materials were washed and dried to determine the amount of crosslinking fraction (CF). The results are shown in **Table 2** and compared with experimental values of DC previously obtained [19-21] calculated by measuring the decrease of the absorption band of coumarin at 320 nm (shown in italic characters).

Table 2. Comparison between crosslinking degree (DC) values obtained by UV experiments and crosslinking fraction (CF) obtained by swelling measurements

Films	**i-PU2KCD5**	**i-PU2KCD5-Si1**	**i-PU2KCD5-mSi1**
DC (UV) (%)	*83*	*95*	*96*
Swelling degree (%)	3600 ± 100	1690 ± 30	1600 ± 300
CF (%)	85 ± 5	93 ± 1	92 ± 1

The incorporation of coumarin within the PU moieties triggers the photo-crosslinking of the polymer matrix allowing its swelling behavior. The swelling degree results clearly show that both SiNPs and coumarin-modified SiNPs restrict the swelling behavior in chloroform, the silica hinders the crystallization degree and provides higher crosslinking degrees in the final materials. The swelling degree data confirms that PU-nanocomposites have higher crosslinking degree than non-reinforced PUs, as it was previously measured by UV spectrophotometry [19, 21]. The swelling behavior with the incorporation of silica nanoparticles into PU matrices was already studied by Kim et al. They found that the incorporation of silica could provide an additional barrier effect on the solvent migration [52]. This effect could be similar in our materials, where both unmodified and modified SiNPs could obstruct the solvent diffusion into the polymer bulk.

The DSC thermograms of all the samples are shown in **Fig. 2**. It is well known that the addition of nanoparticles to the polymer matrix can change its properties in term of crystallinity, mechanical response as well as compatibility between different phases or domains, affecting the shape memory response of the nanocomposites. It was observed that irradiated neat PU (i-PU2K) shows a broad melting transition of PCL crystallites, starting around 30 ºC and reaching the maximum value at 49 ºC (T_m).

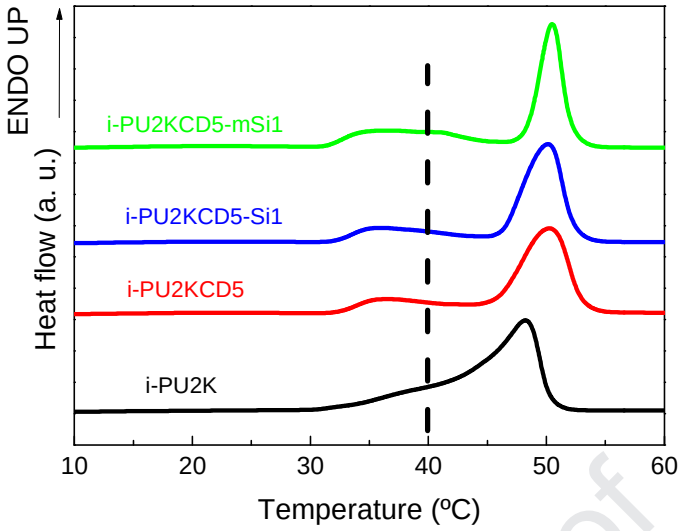

Fig. 2. DSC first heating scan of PU-nanocomposites.

On the other hand, the addition of coumarin moieties within the PU chains, which form a photo-crosslinked network, lead to a different structural distribution of PCL crystallites in the PU matrix. As it is possible to notice in **Fig. 2**, i-PU2KCD5 and its nanocomposites show two melting processes. The first one is characterized by a broad peak with low melting enthalpy, which take place from 30 to 45 ºC and is related to a PCL poorly organized and less stable crystallites. This is probably due to the limitation to SS crystallization by means of the crosslinking network that can locked an amount of soft segment and hinders the good packing of PCL crystallites, promoting the formation of smallest crystallites which melt at lower temperature compared to PCL crystals formed in the neat PU matrix [53]. Therefore, the introduction of coumarin groups and the crosslinking can partially disrupt the order of the soft domain, changing the extent of phase mixing between soft and hard domains [54, 55]. In fact, this phenomenon is clearly reflected in the DSC thermograms where two melting temperatures were detected. The second process is the melting peak related to better organized PCL crystals, which are more stable than that formed in the neat PU showing a higher melting temperature that is shifted from 48 ºC in i-PU2K to 51 ºC in photo-crosslinked materials [20]. Moreover, the addition of both silica nanoparticles, unmodified SiNPs and functionalized mSiNPs, emphasizes

this effect provoking the narrowing of the melting peak, as it is possible to observe in **Fig. 2**, particularly in i-PU2KCD5-mSi1. This behavior has been ascribed to the good interaction between coumarin moieties of PU matrix and SiNPs, which is even better in the case of mSiNPs [19, 21]. In order to thermally-activate the shape memory effect, the presence of two different segments, a hard or permanent segment and a switching or soft segment, which can be influenced by the temperature, is needed. The permanent segment is responsible for retaining the original shape and can be achieved through chemical crosslinking in the polymer network or by a crystalline phase. The switching segment temporarily fixes the programmed shape by a thermally-induced transition or interaction such as the crystallization [56]. In this work, the HS of PU together with the biggest and more stable PCL crystallites act as permanent segment, while the less organized PCL crystallites act as switching segment. Therefore, the T_{trans} used to activate the shape memory response was taken before the melting peak, at 40 ºC. At this temperature, the less thermally stable PCL crystallites melt and the material can be stretched to program its temporary shape. On the other hand, the permanent segments are able to store the elastic strain energy produced during the deformation process, which is the driving force for the shape recovery stage, after the fixation of the temporary shape by freezing at 0 ºC and inducing the crystallization of PCL crystallites. The photo-crosslinking of the network by coumarin moieties dimerization was proposed to increase the stability of the permanent segment and consequently to improve the shape memory properties of the materials. Moreover, the addition of the silica nanoparticles increases the crosslinking degree of the network, as it is showed also for the swelling behavior, and thus it is expected that SiNPs and mSiNPs will improve the ability of the material to retain the original shape of the permanent segment and consequently they will increase the strain recovery ratio. For this reason and in order to verify the shape memory behavior of the developed materials in a first stage, the samples were heated at 40 °C and they were further stretched at 50% of strain to fix the material in a temporary shape. Subsequently,

the films were cooled to 0 °C maintaining the deformation constant. The applied stress was then removed, and the recovery of the original shape occurs by re-heating the samples at the T_{trans}. Thermo-mechanical cycles were performed for neat PU (i-PU2K), photo-crosslinked PU (i-PU2KCD5) and its nanocomposites (i-PU2KCD5-Si1 and i-PU2KCD5-mSi1). 2D strain-stress-temperature-time diagrams are shown in **Fig. 3.** 3D thermo-mechanical strain-stress-temperature cycles and 2D strain-stress diagrams are displayed in **Fig. 4**. Furthermore, the strain-fixity (Rf) and strain-recovery (Rr) ratios are reported in **Table 3**. The samples were programmed in a training cycle (not showed) at the same conditions than cycles 1 and 2.

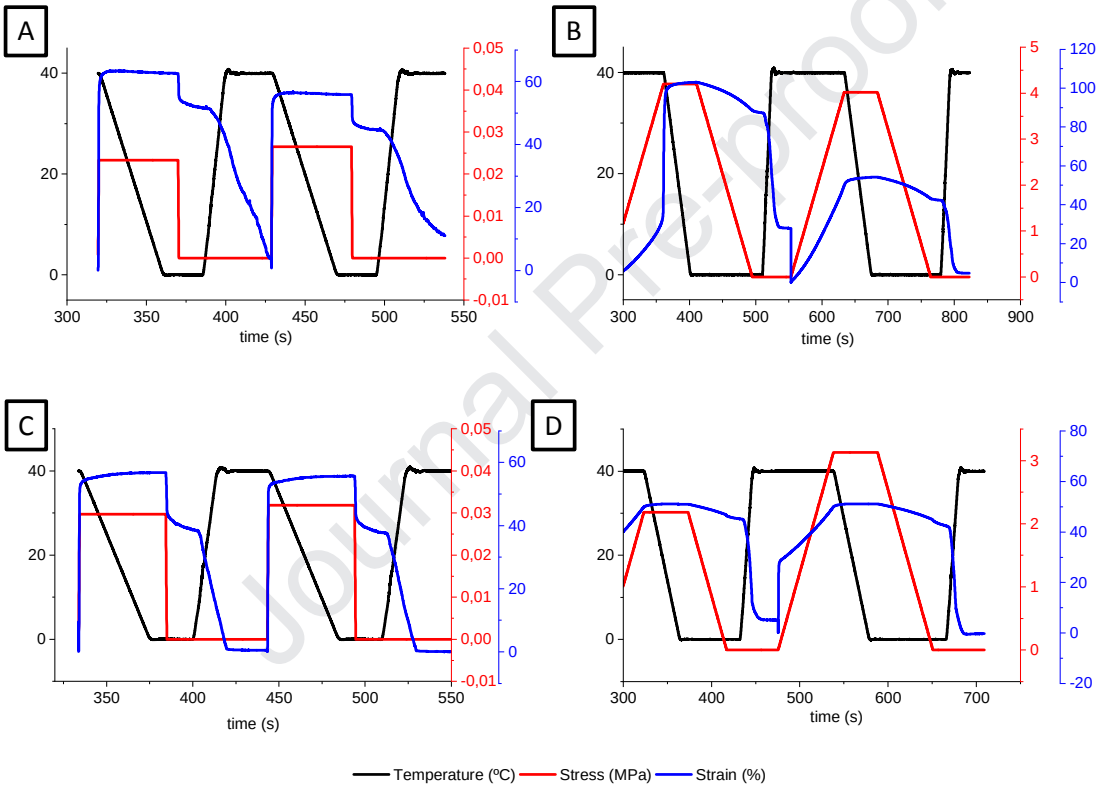

Fig. 3. 2D strain-stress-temperature-time diagrams of **A)** i-PU2K, **B)** i-PU2KCD5, **C)** i-PU2KCD5-Si1, **D)** i-PU2KCD5-mSi1.

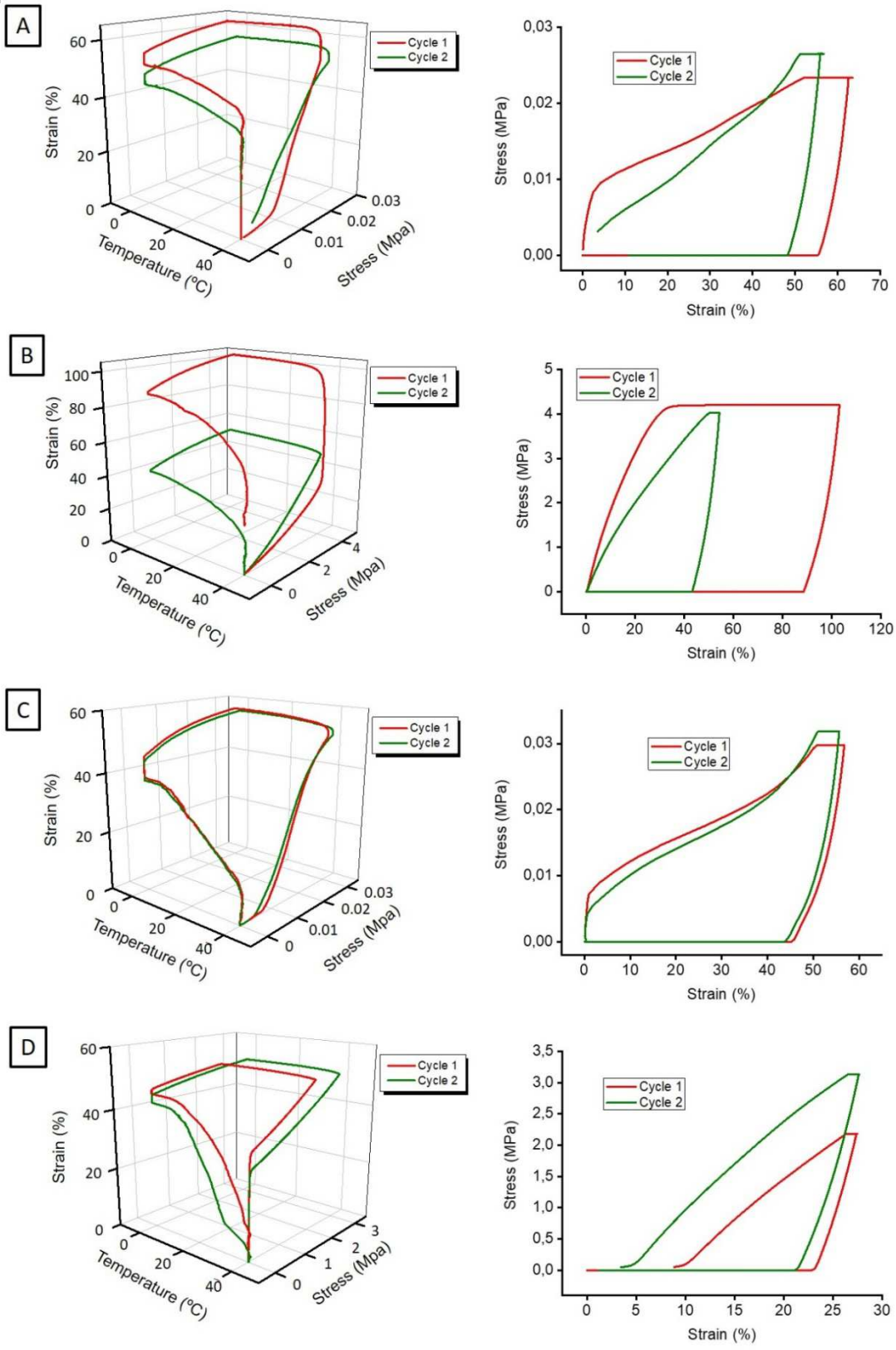

Fig. 4. 3D thermomechanical strain-stress-temperature cycles and 2D stress-strain diagram of **A)** i-PU2K, **B)** i-PU2KCD5, **C)** i-PU2KCD5-Si1, **D)** i-PU2KCD5-mSi1.

Table 3. Values of strain recovery (R_r) and strain fixity ratio (R_f) for the shape memory behavor of photo-crosslinked PU nanocomposites.

	CYCLE			
	R_r		R_f	
SAMPLE	**1**	**2**	**1**	**2**
i-PU2K	99	80	87	83
i-PU2KCD5	73	91	85	78
i-PU2KCD5-Si1	99	100	79	80
i-PU2KCD5-mSi1	90	98	91	87

Firstly, when the films were strained, they showed a stress relaxation recovery typically observed in PUs [57]. Therefore, the recovery ratio was calculated from this point. Neat i-PU2K shows a good shape memory behavior, that is clearly depicted in the **Fig. 4-A**. The film presents a high recovery ratio for the first cycle (99%) (see **Table 3**) and the recuperation begins near to the T_m, caused by the melting of less thermally stable PCL crystallites. However, in the programming cycle, the most of crystallites melted in the PU2K could not be recrystallized again after the cooling; therefore, at the cycle 2 the sample is strained at low values of stress (**Fig 4-A**). On this subject, the incorporation of coumarin and the photo-crosslinking process decreases the crystallinity degree in the PU [19] and consequently, the recovery ratio decreases significantly in the first cycle. The crosslinking process reaches to a higher tensile strength in the i-PU2KCD5 film (**Fig. 4-B**), showing no significantly changes in the fixity ratio regarding to the neat polymer. The difference of strain recovery ratio observed between the cycles 1 and 2 in i-PU2K and i-PU2KCD5 could be explained by the inner stress stored during the film deformation leading to creep [58]. Therefore, the photo-crosslinking network obtained introducing the coumarin moieties did not increase the stability of the permanent segment.

Nevertheless, different situation has been observed for the nanocomposites (**Fig. 4-C and 4-D**). As mentioned in a previous work, the addition of SiNPs enhances the crystal nucleation

during the photo-crosslinking process [19, 21]. The strain recovery ratio is enhanced in the nanocomposites (i-PU2KCD5-Si1 and i-PU2KCD5-mSi1) in comparison with the non-reinforced PUs (i-PU2K and i-PU2KCD5). The unmodified reinforcement (SiNPs) also drives to a slightly decrease in the fixity ratio, probably related with a dissimilar interaction between SiNPs and HS/SS in the PU matrix. In fact, changes in the phase separation have several influences in the mechanical properties. The addition of SiNPs decreases the tensile strength in the PU-nanocomposites, as previously reported [19]. In this sense, the modification of SiNPs allows a higher interaction between the nano-reinforcement and the PU matrix, which stimulates a lower phase separation and a greater stress relaxation in the PU chains, and therefore, enhancing the tensile strength. Therefore, PU2KCD5-mSi shows the best relationship between fixity and recovery ratios.

Finally, to corroborate the biodisintegrable character of the nanocomposites, they were exposed to simulated composting conditions at laboratory scale level. The visual appearance of recovered films at different time of disintegration in composting conditions is shown in **Fig. 5-A**. Meanwhile, the mass loss induced by the composting incubation times is represented in **Fig. 5-B**, where it is clear to observe that the presence of coumarin, besides the hydrophilic nature of SiNPs speed up the overall disintegration process. These results are in agreement with the previously observed for PCL-based nanocomposites reinforced with hydrophilic particles [13, 59].

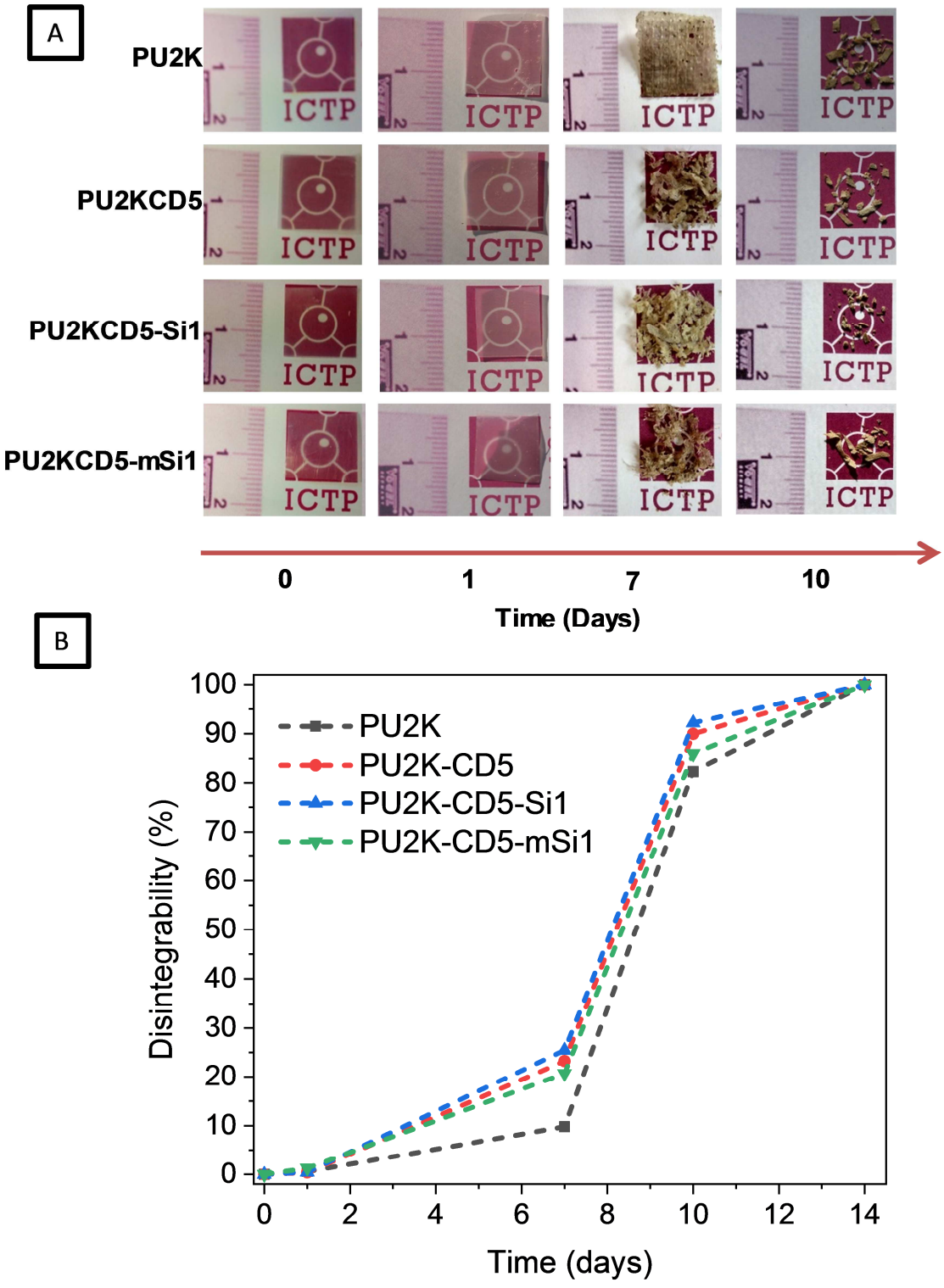

Fig. 5. A) Evolution of PU films visual appearance as well as compost soil before and after different recovered days of disintegration under composting conditions and **B)** Disintegration degree of PU films under composting conditions as a function of time.

Polymer disintegration mainly begins with a hydrolysis process, in which the water diffusion thought the polymer matrix is restricted by the crystallinity of the system, since the ordered structure in the crystalline fraction of the materials could retain the action of microorganisms [60]. In this sense, the less disintegrated material was the neat PU, which showed the highest crystallinity degree (X_c = 31%) with regard to the already reported crystallinity of coumarin based PUs (X_c between 26 - 27%) [21]. Concerning the photo-crosslinked polyurethanes, the disintegrability degree shows similar diminishing tendency to the surface wettability [21]. In fact, PU2KCD5-Si1 sample showed the most hydrophilic surface (water contact angle = 71± 1º) [21] and the higher rate of disintegration.

After 7 days in composting conditions, the characteristic high transparency of PCL-based PUs [45] decreased and films became opaque as a consequence of the changes in the polymer matrices refraction index, owing to the water absorption and/or the presence of products formed by the hydrolytic degradation process [61, 62]. At this stage of disintegration, the materials were opaque and acquired increasing yellow-brown tonality.

The disintegration process was further assessed by SEM (**Fig. 6**). The initial PU2K microstructural surface was smooth and non-porous (**Fig. 6-A**), while it became slightly more porous after 7 days in compost medium showing some signs of disintegration (**Fig. 6-B**), in accordance with the significant macroscopic changes observed at this disintegration stage (**Fig. 5-A**).

At 10 days of disintegration, small dark brown pieces were recovered (**Fig. 5-A**). Finally, after 14 days the samples reached the goal of disintegrability test (90% of disintegration according to ISO 20200) (**Fig. 5-B**). The evolution of compost medium showed changes during the composting test; resulting in a dark humus soil due to the aerobic fermentation (not shown) [63].

Coumarin-based PUs are more disintegrated at 7 days of disintegration test. In fact, they became in breakable and small pieces (**Fig. 5-A**). More porous surfaces were initially observed

by SEM analysis for coumarin-based PUs (PU2KCD5 **Fig. 6-C**) and nanocomposites (PU2KCD5-Si1 **Fig. 6-E** and **Fig. 6-G**), which after 7 days in the compost medium showed higher microstructural signs of disintegration, in agreement with the higher mass loss (**Fig. 5-B**), such as a marked increase in the surface roughness for PU2KCD5 (**Fig. 6-D**)**.** In the case of nanocomposites, they showed more degraded areas with cavities (**Fig. 6-F** and **Fig. 6-H**), which imply a non-homogeneous mechanism for the degradation process. This phenomenon has been previously observed and was attributed to better contact of the compost in the most degraded areas and/or to a non-homogeneous growth of the microorganisms on the sample surface [61].

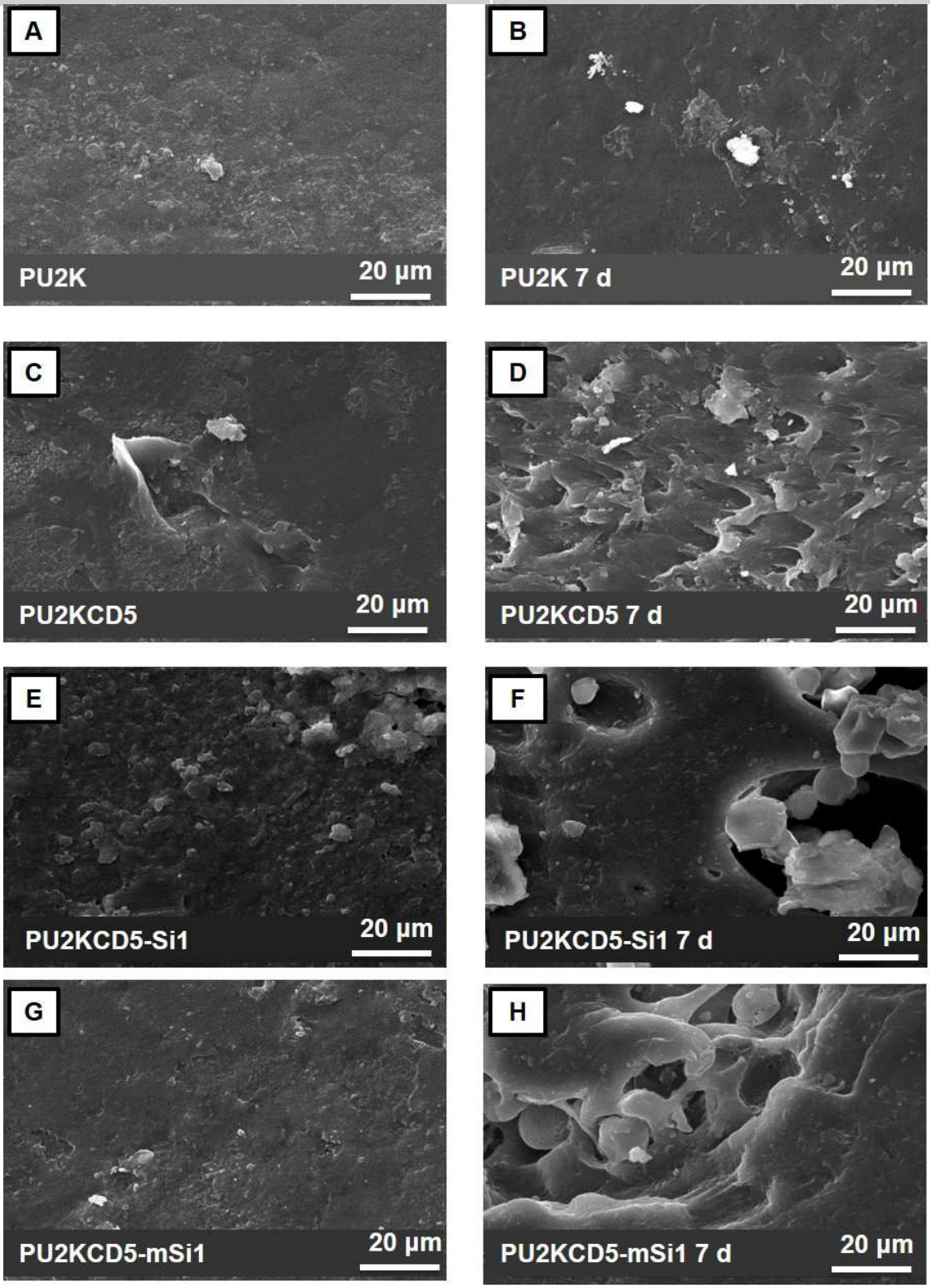

Fig. 6. SEM pictures of PU films before and after 7 days of disintegration under composting conditions.

The **Fig. 7** shows the FTIR spectra of coumarin-based PU films before and after 7 days in composting conditions. An intensity increase was observed in the region of –OH and –NH stretch (3600-3000 cm^{-1}), related with a disintegration process of the urethane bonds, which

resulted particularly intense in the case of neat PU film (**Fig. 7-A**). This intensity increase is followed by an increase of the signal at 1650 cm^{-1} (see **Fig. 7-B**), belonging to the asymmetric stretching vibration of carboxylate ions [62, 64]. The increase of these bands reveals the typically disintegration behavior of PCL-based PUs [45]. Moreover, the increase of the O-H stretching signals, corresponding to the carboxylic end groups, is considerably enhanced in the PU2K in comparison with coumarin-based PUs (**Fig. 7-C**) and its nanocomposites (**Fig. 7-G and 7-E**), suggesting that in the neat PU, the degradation take place via hydrolytic rupture of both urethane and ester linkages. This can be corroborated by the decrease of the bands at 1730 cm^{-1} (C=O stretching) and at 1239 cm^{-1} (asymmetric C-O-C stretching).

A different behavior is presented in the sample PU2KCD5 (**Fig. 7-C** and **7-D**), which shows a smaller increase of the O-H stretching band than neat PU. The lower amount of free –OH (3600-3000 cm^{-1}) are probably forming hydrogen bonding interactions with the carbonyl groups of coumarin.

The addition of both SiNPs (**Fig. 7-E** and **7-F**) and modified SiNPs (**Fig. 7-G** and **7-H**) leads to a less increase of the –OH stretch band. There is also a higher decrease of the bands at 1730 cm^{-1} (C=O stretching) and at 1239 cm^{-1} (asymmetric C-O-C stretching) in comparison with the sample PU2KCD5 corroborating that disintegration process is enhanced by the presence of the nanoparticles within the PU matrix.

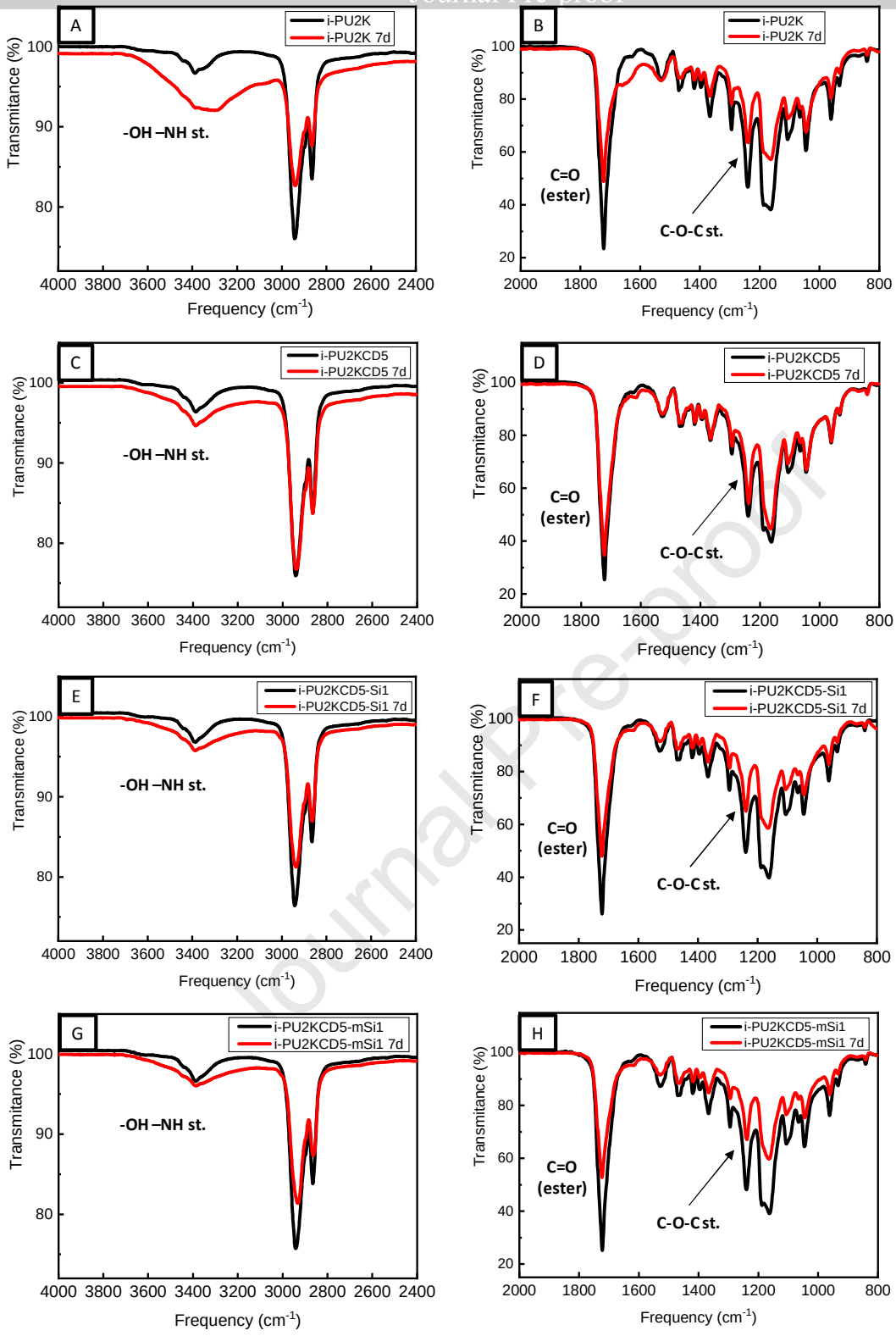

Fig 7. FTIR spectra before and after 7 days of disintegration under composting conditions of: PU2K A) 4000–2400 cm^{-1} and B) 2000–800 cm^{-1}; PU2KCD5 C) 4000–2400 cm^{-1} and D) 2000–800 cm^{-1}; PU2KCD5-Si1 E) 4000–2400 cm^{-1} and F) 2000–800 cm^{-1}; PU2KCD5-mSi1 G) 4000–2400 cm^{-1} and H) 2000–800 cm^{-1}.

3 Conclusions

In this manuscript, stimuli responsive properties of photo-crosslinked coumarin-based PUs and their nanocomposites were assessed. The study of the swelling behavior confirmed the crosslinking degree previously calculated by UV-measurements. Thermally-activated shape memory properties were studied by thermo-mechanical cycles. The HS of PUs together with the biggest and more stable PCL crystallites acted as permanent segment retaining the original shape, while the smallest PCL crystallites acted as switching segment and fixed the temporary shape. All the samples showed good shape memory properties, displaying maximum R_r values of 100% and R_f values higher than 80%. Particularly, PU with coumarin-based silica nanoparticles showed the highest strain fixity and strain recovery ratios leading to the best shape memory performance for i-PU2KCD5-mSi nanocomposite. The biodisintegration test under composting conditions revealed that SiNPs enhance the disintegration of the PU matrix. This information can provide a better knowledge to the development of coatings with tunable properties and sustainable end-life option.

4 Acknowledgements

Authors thank Spanish Ministry of Economy, Industry and Competitiveness, MINEICO (MAT2016-MAT2016-78437-R, MAT2017-88123-P, PCIN-2017-036), the Agencia Estatal de Investigación (AEI, Spain), and Fondo Europeo de Desarrollo Regional (FEDER, EU). M.P.A. and L.P. acknowledge the Juan de la Cierva (FJCI-2014-20630) and Ramon y Cajal (RYC-2014-15595) contracts from the MINEICO, respectively. V.S. thanks the Wallonia Region, West-Vlaanderen Region, Agentschap Innoveren Ondernemen and European Community (FEDER funds) for the financial support in the frame of the INTERREG V FWVL – BIOHARV project (GoToS3 portofolio).

5 References

[1] G. Kaur, P. Johnston, K. Saito, Photo-reversible dimerisation reactions and their applications in polymeric systems, Polymer Chemistry, 5 (2014) 2171-2186.

[2] N. Kuş, S. Breda, I. Reva, E. Tasal, C. Ogretir, R. Fausto, FTIR Spectroscopic and Theoretical Study of the Photochemistry of Matrix□isolated Coumarin, Photochemistry and photobiology, 83 (2007) 1237-1253.

[3] T. Wolff, H. Görner, Photocleavage of dimers of coumarin and 6-alkylcoumarins, Journal of Photochemistry and Photobiology A: Chemistry, 209 (2010) 219-223.

[4] J. Donovalová, M. Cigáň, H. Stankovičová, J. Gašpar, M. Danko, A. Gáplovský, P. Hrdlovič, Spectral properties of substituted coumarins in solution and polymer matrices, Molecules, 17 (2012) 3259-3276.

[5] K. Gnanaguru, N. Ramasubbu, K. Venkatesan, V. Ramamurthy, A study on the photochemical dimerization of coumarins in the solid state, The Journal of Organic Chemistry, 50 (1985) 2337-2346.

[6] D.H. Qu, Q.C. Wang, Q.W. Zhang, X. Ma, H. Tian, Photoresponsive Host-Guest Functional Systems, Chemical Reviews, 115 (2015) 7543-7588.

[7] J.K. Chen, C.J. Chang, Fabrications and applications of stimulus-responsive polymer films and patterns on surfaces: A review, Materials, 7 (2014) 805-875.

[8] J.M. Cuevas, R. Seoane-Rivero, R. Navarro, Á. Marcos-Fernández, Coumarins into Polyurethanes for Smart and Functional Materials, Polymers, 12 (2020) 630.

[9] M.R. Williamson, R. Black, C. Kielty, PCL–PU composite vascular scaffold production for vascular tissue engineering: Attachment, proliferation and bioactivity of human vascular endothelial cells, Biomaterials, 27 (2006) 3608-3616.

[10] X. Jiang, J. Li, M. Ding, H. Tan, Q. Ling, Y. Zhong, Q. Fu, Synthesis and degradation of nontoxic biodegradable waterborne polyurethanes elastomer with poly (ε-caprolactone) and poly (ethylene glycol) as soft segment, European Polymer Journal, 43 (2007) 1838-1846.

[11] Z. Tang, R. Black, J. Curran, J. Hunt, N. Rhodes, D. Williams, Surface properties and biocompatibility of solvent-cast poly [ε-caprolactone] films, Biomaterials, 25 (2004) 4741-4748.

[12] I. Navarro-Baena, M.P. Arrieta, A. Sonseca, L. Torre, D. López, E. Giménez, J.M. Kenny, L. Peponi, Biodegradable nanocomposites based on poly (ester-urethane) and nanosized hydroxyapatite: plastificant and reinforcement effects, Polymer Degradation and Stability, 121 (2015) 171-179.

[13] M. Arrieta, V. Sessini, L. Peponi, Biodegradable poly (ester-urethane) incorporated with catechin with shape memory and antioxidant activity for food packaging, European Polymer Journal, 94 (2017) 111-124.

[14] J. De Groot, R. De Vrijer, B. Wildeboer, C. Spaans, A. Pennings, New biomedical polyurethane ureas with high tear strengths, Polymer Bulletin, 38 (1997) 211-218.

[15] H.M. Nakhoda, Y. Dahman, Mechanical properties and biodegradability of porous polyurethanes reinforced with green nanofibers for applications in tissue engineering, Polymer Bulletin, 73 (2016) 2039-2055.

[16] A. Khosravi, M. Sadeghi, H.Z. Banadkohi, M.M. Talakesh, Polyurethane-silica nanocomposite membranes for separation of propane/methane and ethane/methane, Industrial & Engineering Chemistry Research, 53 (2014) 2011-2021.

[17] M.P. Arrieta, L. Peponi, Polyurethane based on PLA and PCL incorporated with catechin: Structural, thermal and mechanical characterization, European Polymer Journal, 89 (2017) 174-184.

[18] H. Deka, N. Karak, Bio-based hyperbranched polyurethanes for surface coating applications, Progress in Organic Coatings, 66 (2009) 192-198.

[19] C. Salgado, M.P. Arrieta, L. Peponi, M. Fernández-García, D. López, Silica-nanocomposites of photo-crosslinkable poly (urethane) s based on poly (ε-caprolactone) and coumarin, European Polymer Journal, 93 (2017) 21-32.

[20] C. Salgado, M.P. Arrieta, L. Peponi, M. Fernández□García, D. López, Influence of Poly (ε□caprolactone) Molecular Weight and Coumarin Amount on Photo□Responsive Polyurethane Properties, Macromolecular Materials and Engineering, 302 (2017) 1600515.

[21] C. Salgado, M.P. Arrieta, L. Peponi, D. López, M. Fernández-García, Photo-crosslinkable polyurethanes reinforced with coumarin modified silica nanoparticles for photo-responsive coatings, Progress in Organic Coatings, 123 (2018) 63-74.

[22] G. Chen, S. Zhou, G. Gu, L. Wu, Modification of colloidal silica on the mechanical properties of acrylic based polyurethane/silica composites, Colloids and Surfaces A: Physicochemical and Engineering Aspects, 296 (2007) 29-36.

[23] G. Chen, S. Zhou, G. Gu, H. Yang, L. Wu, Effects of surface properties of colloidal silica particles on redispersibility and properties of acrylic-based polyurethane/silica composites, Journal of colloid and interface science, 281 (2005) 339-350.

[24] H.J. Jeon, J.S. Kim, T.G. Kim, J.H. Kim, W.-R. Yu, J.H. Youk, Preparation of poly (ε-caprolactone)-based polyurethane nanofibers containing silver nanoparticles, Applied Surface Science, 254 (2008) 5886-5890.

[25] M. Sadeghi, M.M. Talakesh, B. Ghalei, M. Shafiei, Preparation, characterization and gas permeation properties of a polycaprolactone based polyurethane-silica nanocomposite membrane, Journal of membrane science, 427 (2013) 21-29.

[26] J.-M. Yeh, C.-T. Yao, C.-F. Hsieh, H.-C. Yang, C.-P. Wu, Preparation and properties of amino-terminated anionic waterborne-polyurethane–silica hybrid materials through a sol–gel process in the absence of an external catalyst, European Polymer Journal, 44 (2008) 2777-2783.

[27] Y. Duan, S.C. Jana, B. Lama, M.P. Espe, Reinforcement of silica aerogels using silane-end-capped polyurethanes, Langmuir, 29 (2013) 6156-6165.

[28] S. Li, R. Vatanparast, H. Lemmetyinen, Cross-linking kinetics and swelling behaviour of aliphatic polyurethane, Polymer, 41 (2000) 5571-5576.

[29] K. Mequanint, A. Patel, D. Bezuidenhout, Synthesis, Swelling Behavior, and Biocompatibility of Novel Physically Cross-Linked Polyurethane-block-Poly(glycerol methacrylate) Hydrogels, Biomacromolecules, 7 (2006) 883-891.

[30] Y. Chujo, K. Sada, T. Saegusa, Polyoxazoline having a coumarin moiety as a pendant group. Synthesis and photogelation, Macromolecules, 23 (1990) 2693-2697.

[31] M.A. Azagarsamy, D.D. McKinnon, D.L. Alge, K.S. Anseth, Coumarin-based photodegradable hydrogel: Design, synthesis, gelation, and degradation kinetics, ACS Macro Letters, 3 (2014) 515-519.

[32] M. Barikani, C. Hepburn, Determination of crosslink density by swelling in the castable polyurethane elastomer based on 1/4 - cyclohexane diisocyanate and para-phenylene diisocyanate, 1992.

[33] V. Sessini, J.-M. Raquez, G. Lo Re, R. Mincheva, J.M. Kenny, P. Dubois, L. Peponi, Multiresponsive Shape Memory Blends and Nanocomposites Based on Starch, ACS Applied Materials & Interfaces, 8 (2016) 19197-19201.

[34] V. Sessini, M.P. Arrieta, A. Fernández-Torres, L. Peponi, Humidity-activated shape memory effect on plasticized starch-based biomaterials, Carbohydrate Polymers, 179 (2018) 93-99.

[35] X.J. Han, Z.Q. Dong, M.M. Fan, Y. Liu, J.H. li, Y.F. Wang, Q.J. Yuan, B.J. Li, S. Zhang, pH□induced shape□memory polymers, Macromolecular rapid communications, 33 (2012) 1055-1060.

[36] D. Habault, H. Zhang, Y. Zhao, Light-triggered self-healing and shape-memory polymers, Chemical Society Reviews, 42 (2013) 7244-7256.

[37] L. Peponi, V. Sessini, M.P. Arrieta, I. Navarro-Baena, A. Sonseca, F. Dominici, E. Gimenez, L. Torre, A. Tercjak, D. López, Thermally-activated shape memory effect on biodegradable nanocomposites based on PLA/PCL blend reinforced with hydroxyapatite, Polymer Degradation and Stability, 151 (2018) 36-51.

[38] J. Lin, L. Chen, Study on shape□memory behavior of polyether□based polyurethanes. I. Influence of the hard□segment content, Journal of applied polymer science, 69 (1998) 1563-1574.

[39] B.K. Kim, S.Y. Lee, M. Xu, Polyurethanes having shape memory effects, Polymer, 37 (1996) 5781-5793.

[40] J. Hu, Z. Yang, L. Yeung, F. Ji, Y. Liu, Crosslinked polyurethanes with shape memory properties, Polymer International, 54 (2005) 854-859.

[41] C.-H. Wu, S.-M. Shau, S.-C. Liu, S.A. Dai, S.-C. Chen, R.-H. Lee, C.-F. Hsieh, R.-J. Jeng, Enhanced shape memory performance of polyurethanes via the incorporation of organic or inorganic networks, RSC Advances, 5 (2015) 16897-16910.

[42] J.W. Cho, J.W. Kim, Y.C. Jung, N.S. Goo, Electroactive shape□memory polyurethane composites incorporating carbon nanotubes, Macromolecular rapid communications, 26 (2005) 412-416.

[43] I. Navarro-Baena, J.M. Kenny, L. Peponi, Thermally-activated shape memory behaviour of bionanocomposites reinforced with cellulose nanocrystals, Cellulose, 21 (2014) 4231-4246.

[44] I.S. Gunes, F. Cao, S.C. Jana, Evaluation of nanoparticulate fillers for development of shape memory polyurethane nanocomposites, Polymer, 49 (2008) 2223-2234.

[45] M.P. Arrieta, K.A.B. Rivera, C. Salgado, A.M. Richa, D. López, L. Peponi, Degradation under composting conditions of lysine-modified polyurethane based on PCL obtained by lipase biocatalysis, Polymer Degradation and Stability, 152 (2018) 139-146.

[46] R. Seoane Rivero, R. Navarro, P. Bilbao Solaguren, K. Gondra Zubieta, J.M. Cuevas, A. Marcos-Fernández, Synthesis and characterization of photo-crosslinkable linear segmented polyurethanes based on coumarin, European Polymer Journal, 92 (2017) 263-274.

[47] M.D. Stelescu, E. Manaila, G. Craciun, N. Zuga, Crosslinking and grafting ethylene vinyl acetate copolymer with accelerated electrons in the presence of polyfunctional monomers, Polymer Bulletin, 68 (2012) 263-285.

[48] J. Dong, R.A. Weiss, Effect of Crosslinking on Shape-Memory Behavior of Zinc Stearate/Ionomer Compounds, Macromolecular Chemistry and Physics, 214 (2013) 1238-1246.

[49] P. Ma, D.G. Hristova-Bogaerds, P.J. Lemstra, Y. Zhang, S. Wang, Toughening of PHBV/PBS and PHB/PBS Blends via In situ Compatibilization Using Dicumyl Peroxide as a Free-Radical Grafting Initiator, Macromolecular Materials and Engineering, 297 (2012) 402-410.

[50] U.-E. ISO, ISO 20200:2015. Plastics. Determination of the degree of disintegration of plastic materials under simulated composting conditions in a laboratory-scale test, (2016).

[51] M.P. Arrieta, J. López, A. Hernández, E. Rayón, Ternary PLA–PHB–Limonene blends intended for biodegradable food packaging applications, European Polymer Journal, 50 (2014) 255-270.

[52] B.S. Kim, S.H. Park, B.K. Kim, Nanosilica-reinforced UV-cured polyurethane dispersion, Colloid and Polymer Science, 284 (2006) 1067-1072.

[53] J.-L. Chen, F.-C. Chang, Phase separation and melting behavior in poly(ε-caprolactone)-epoxy blends cured by 3,3′-dimethylmethylene-di(cyclohexylamine), Journal of applied polymer science, 89 (2003) 3107-3114.

[54] Y. Zhu, J. Hu, K.f. Choi, Q. Meng, S. Chen, K.w. Yeung, Shape memory effect and reversible phase crystallization process in SMPU ionomer, Polymers for Advanced Technologies, 19 (2008) 328-333.

[55] A. Güney, N. Hasirci, Properties and phase segregation of crosslinked PCL□based polyurethanes, Journal of applied polymer science, 131 (2014).

[56] S. Thakur, J. Hu, Polyurethane: A Shape Memory Polymer (SMP), in: Aspects of Polyurethanes, IntechOpen, 2017.

[57] X. Gu, P.T. Mather, Entanglement-based shape memory polyurethanes: Synthesis and characterization, Polymer, 53 (2012) 5924-5934.

[58] P. Ping, W. Wang, X. Chen, X. Jing, Poly(ε-caprolactone) Polyurethane and Its Shape-Memory Property, Biomacromolecules, 6 (2005) 587-592.

[59] V. Sessini, I. Navarro-Baena, M.P. Arrieta, F. Dominici, D. López, L. Torre, J.M. Kenny, P. Dubois, J.-M. Raquez, L. Peponi, Effect of the addition of polyester-grafted-cellulose nanocrystals on the shape memory properties of biodegradable PLA/PCL nanocomposites, Polymer Degradation and Stability, 152 (2018) 126-138.

[60] M.P. Arrieta, M.D. Samper, M. Aldas, J. López, On the use of PLA-PHB blends for sustainable food packaging applications, Materials, 10 (2017).

[61] K. Fukushima, D. Tabuani, C. Abbate, M. Arena, L. Ferreri, Effect of sepiolite on the biodegradation of poly(lactic acid) and polycaprolactone, Polymer Degradation and Stability, 95 (2010) 2049-2056.

[62] E. Fortunati, I. Armentano, A. Iannoni, M. Barbale, S. Zaccheo, M. Scavone, L. Visai, J. Kenny, New multifunctional poly (lactide acid) composites: mechanical, antibacterial, and degradation properties, Journal of applied polymer science, 124 (2012) 87-98.

[63] M.P. Arrieta, E. Fortunati, F. Dominici, E. Rayón, J. López, J.M. Kenny, PLA-PHB/cellulose based films: Mechanical, barrier and disintegration properties, Polymer Degradation and Stability, 107 (2014) 139-149.

[64] M.P. Arrieta, J. López, E. Rayón, A. Jiménez, Disintegrability under composting conditions of plasticized PLA–PHB blends, Polymer Degradation and Stability, 108 (2014) 307-318.

Highlights

- Functional polyurethanes based on poly-e-caprolactone and coumarin have been evaluated as coatings.
- Photo-crosslinking degree was measured by swelling and the results are in concordance with UV measurements.
- The incorporation of coumarin-functionalized silica nanoparticles leads to a enhancement of the shape memory performance.
- The nanocomposites were completely disintegrated after 14 days under composting conditions.

Declaration of interests

☒ The authors declare that they have no known competing financial interests or personal relationships that could have appeared to influence the work reported in this paper.

☐The authors declare the following financial interests/personal relationships which may be considered as potential competing interests: